J Mol Model (2013) 19:4959–4967
DOI 10.1007/s00894-013-1993-7

ORIGINAL PAPER

Effect of surface hydroxyls on dimethyl ether synthesis over the γ-Al_2O_3 in liquid paraffin: a computational study

Zhi-jun Zuo · Le Wang · Pei-de Han · Wei Huang

Received: 22 July 2013 / Accepted: 29 August 2013 / Published online: 22 September 2013

Abstract In a recent paper (Zuo et al., Appl Catal A 408:130–136, 2011), the mechanism of dimethyl ether (DME) synthesis from methanol dehydration over γ-Al_2O_3 (110) was studied using density functional theory (DFT). Using the same method, the effect of surface hydroxyls on γ-Al_2O_3 in liquid paraffin during DME synthesis from methanol dehydration is investigated. It is found that DME is mainly formed from two adsorbed CH_3O groups via methanol dehydrogenation on both dehydrated and hydrated γ-Al_2O_3 in liquid paraffin. No close correlation between catalytic activity and acid intensity was found. Before and after water adsorption at typical catalytic conditions (e.g., 553 K), the reaction rate is not obviously changed on γ-Al_2O_3(100) surface in liquid paraffin, but the reaction rate decreases by about 11 times on the (110) in liquid paraffin. Considering the area of the (110) and (100) surfaces under actual conditions, the catalytic activity decreased mainly because the Al3 sites on the (110) surface gradually become inactive. Catalytic activity decreased mainly due to surface hydrophilicity. The calculated results were consistent with the experiment.

Keywords DFT · DME · Liquid paraffin · Methanol · γ-Al_2O_3

Z.-j. Zuo · L. Wang · W. Huang (✉)
Key Laboratory of Coal Science and Technology of Ministry of Education and Shanxi Province, Taiyuan, Shanxi, China
e-mail: huangwei@tyut.edu.cn

P.-d. Han
College of Materials Science and Engineering, Taiyuan University of Technology, Taiyuan 030024, Shanxi, China

Introduction

Dimethyl ether (DME) synthesis has recently attracted increased attention because of its low NO_x emission and non-corrosiveness [1, 2]. It can be produced from syngas over a bi-functional catalyst, such as Cu/Zn/γ-Al_2O_3 [3–5]. The slurry bed has the following advantages low gas recycling ratio, no diffusion limitations, low pressure drop over the reactor, and caloric transfer [6]. Therefore, the slurry reactor has attracted more attention in DME synthesis from syngas [7–11]. The catalyst is dispersed in an inert liquid medium, such as liquid paraffin, in a slurry reactor, during which γ-Al_2O_3 is used for methanol dehydration [6–11]. DME is generally synthesized from methanol dehydration via the reaction $2CH_3OH \rightarrow CH_3OCH_3 + H_2O$ [12, 13]. In our previous studies, we showed that CH_3OH undergoes dissociative adsorption on the γ-Al_2O_3 surface and DME is formed by the reaction of two CH_3O groups [14]. In these works, water was observed to be the main by-product. In liquid paraffin, the activity of γ-Al_2O_3 decreases as reaction time increases, and some researchers propose that water decreases the activity of γ-Al_2O_3 acid by its high adsorption capacity on acid sites [15–17].

γ-Al_2O_3 is commonly used as a catalyst/support because of its fine particle size, large surface area, excellent thermal stability, high mechanical resistance, and wide range of chemical, physical, and catalytic properties [18–20]. Raybaud et al. [20–22] and Ionescu et al. [23] proposed that non-dissociative and dissociative adsorptions of water occur over the Lewis acid sites of the γ-Al_2O_3 surface, indicating that the amount of water may influence catalytic activity during DME synthesis from methanol dehydration. Studies show that the γ-Al_2O_3 surface is inevitably hydrated/hydroxylated under realistic reaction conditions. The influence of surface hydroxyls over γ-Al_2O_3 has been studied using theoretical methods [24–27]. For example, Pan et al. [24] studied the effect of surface hydroxyls on selective CO_2 hydrogenation over Ni/γ-Al_2O_3. The intermediates found on the dehydrated and the hydroxylated γ-Al_2O_3 (110) surfaces were HCOO and CO, respectively, indicating that hydroxylation of γ-Al_2O_3 supports can alter the pathway and selectivity of CO_2 hydrogenation. Zhang et al. [25] also studied the effect of surface hydroxyls on selective CO_2 hydrogenation over Cu/γ-Al_2O_3 and found that hydroxylation of the γ-Al_2O_3 support cannot alter the pathway of CO_2 hydrogenation; the selectivity of CO_2 hydrogenation for HCOO formation on Cu/γ-Al_2O_3 was also high. In our previous study, it is found that water adsorption on γ-Al_2O_3 surface will influence the adsorptive behavior of methanol and DME [27].

How does water influence DME synthesis from methanol dehydration over a γ-Al_2O_3 catalyst in a slurry reactor? Although water is the main product of the catalytic reaction, few studies about the effect of hydroxylation of the γ-Al_2O_3 catalysts on the DME synthesis from methanol dehydration have been conducted. To better understand the effect of water adsorption during DME synthesis on a γ-Al_2O_3 surface in a slurry reactor, we performed DFT calculations on a conductor-like solvent model (COSMO) and studied methanol dehydration on γ-Al_2O_3 as influenced by water in the presence of liquid paraffin, which is always used as a insert medium in the liquid paraffin. A close relation between the dehydrated and hydrated γ-Al_2O_3 in liquid paraffin and the corresponding reaction processes was found.

Computational models and methods

Computational models

Researchers have proposed that γ-Al_2O_3 models include the defective spinel model and the non-spinel model [20, 28–31]. Because the non-spinel model agrees well with experimental data (i.e., NMR, XRD, and IR), it is used in the present paper to create surfaces as in previous studies [20, 32]. Experimental results show that the γ-Al_2O_3 (110) and (100) surfaces predominate 83 % and 17 % of the total surface, respectively [33]. Thus, the two main orientations under actual catalytic conditions, the (100) and (110) surfaces, were considered.

To minimize the interaction of adsorbates of neighboring slabs, supercells of (1×2) and (2×1) were chosen for the γ-Al_2O_3 (110) and (100) surfaces, respectively. The supercells contained 24 and 16 Al_2O_3 units, respectively. The last two slabs of the γ-Al_2O_3 (110) and (100) surfaces were frozen in their bulk positions whereas the other slabs and adsorbates were fully relaxed. The vacuum zone between the slabs was set to 15 Å.

To describe the interaction between the adsorbates and the γ-Al_2O_3 (hkl) in liquid paraffin, the adsorption energy (E_{ads}) was defined as [34]:

$$E_{ads} = E(adsorbate/slab) - [E(adsorbate) + E(slab)],$$

where E(adsorbate/slab), E(adsorbate), and E(slab) are the total energies of the slab with the adsorbate on its surface, of the free adsorbate, and of the slab surface, respectively. A negative E_{ads} value signifies an exothermic adsorption and a positive E_{ads} value indicates an endothermic adsorption. The reaction energy (ΔH), like A + B = C + D, was calculated as [35]:

$$\Delta H = [E(C/slab) + E(D/slab)] - [E(A/slab) + E(B/slab)],$$

where E(C/slab), E(D/slab) and E(A/slab), E(B/slab) are the total energies of the slab with products and reactants on its surface, respectively. A negative ΔH value signifies an exothermic reaction and a positive ΔH value indicates an endothermic reaction.

Computational methods

The unrestricted density functional calculations were conducted using the $DMol^3$ program package in Materials Studio 5.5 [36, 37]. The calculation is conducted with the generalized gradient approximation with the Perdew–Wang exchange–correlation functional (GGA-PW91) [38], and the electron-ion interaction was described using DFT semi-core pseudopots (DSPP) [39, 40]. The double numerical atomic orbital basis set plus polarization function (DNP) [39] was also used. All calculations with a k-point grid of (2×2×1) and (2×2×1) gave a numerical difference in γ-Al_2O_3 (110) and (100) surfaces energy of less than 0.001 eV.

To simulate γ-Al_2O_3 in liquid paraffin, the conductor-like screening model (COSMO) implemented in $Dmol^3$ was used [41, 42]. COSMO is a continuum solvent model where the solute molecule forms a cavity within the dielectric continuum of permittivity, ε, that represents the solvent [43–45]. The charge distribution of the solute polarizes the dielectric medium. The response of the dielectric medium is described by the generation of screening (or polarization) charges on the cavity surface. These charges are then scaled by a factor $f(\varepsilon) = (\varepsilon - 1)/(\varepsilon + 0.5)$ to obtain a rather favorable approximation of the screening charges in a dielectric medium. The dielectric constant of liquid paraffin was set to 2.06.

Transition states (TS) were searched using the complete LST/QST method [46]. Linear synchronous transit (LST) maximization was performed, followed by energy minimization in the directions conjugating to the reaction pathway. The approximated TS values were used for quadratic synchronous transit (QST) maximization. From this point, another

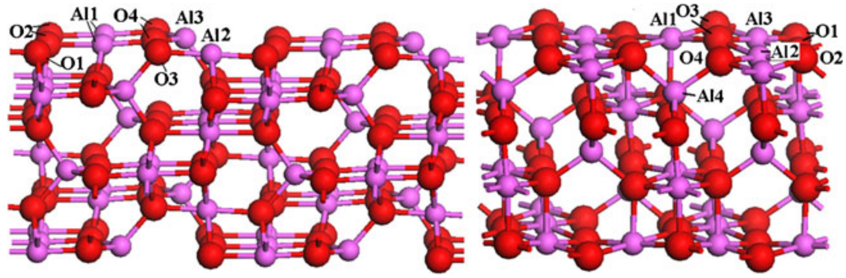

Fig. 1 Side views of the dehydrated γ-Al_2O_3(110)(*left*) and (100)(*right*) in liquid paraffin. *Light gray* and *gray spheres* represent Al and O, respectively

conjugate gradient minimization was performed. The cycle was repeated until a stationary point was located [47].

Results and discussion

The side views of the dehydrated γ-Al_2O_3 (110) and (100) in liquid paraffin are shown in Fig. 1. According to the coordination of the atoms, unsaturated Al and O atoms comprise the Lewis acid and base sites, respectively. Previous studies show that DME synthesis from methanol occurs over Lewis acid sites [20, 48–50]. Thus, in the present study, only Al sites were considered. The (110) surface exhibited two kinds of unsaturated aluminum surface sites. Al3 was three-fold coordinated. Al1 and Al2 atoms were four-fold coordinated but showed different chemical environments. As for γ-Al_2O_3 (100) surface, Al4 is four-fold coordinated and in a position below the surface plane, therefore, it is not available for adsorption. Al1 ~ Al3 atoms are five-fold coordinated, however, Al1 ~ Al3 atoms are different in the chemical environments. Thus, we only consider DME and methanol adsorption over Al1 ~ Al3 sites. The detail sees ref [14, 27].

The adsorptive behavior of water on the γ-Al_2O_3 (hkl) surface was studied by Raybaud et al. in detail [20, 28], who found that the (100) surface is completely dehydrated above 873 °C whereas the (111) surface remains fully hydrated up to about 1073 °C. Even at 1273 °C, the hydroxyl coverage was still high (9.8 OH nm^{-2}). When the temperature was around 280 °C, the OH concentrations on the (110) and (100) surfaces were 8.9 and 4.3 OH nm^{-2}, respectively. In actual reaction systems of DME synthesis from methanol over γ-Al_2O_3 catalysts, the reaction temperature is within the temperature range of 230 and 290 °C. Thus, (110) and (100) surfaces with OH concentrations of 8.9 and 4.3 OH nm^{-2} were studied.

Figure 2 shows the side views of the hydrated γ-Al_2O_3 (110) and the (100) in liquid paraffin. On γ-Al_2O_3 (110) in liquid paraffin, the Al3 site has an adsorbed OH group, two Al1 sites share one bridge-like OH group, and the Al2 site has one adsorbed H_2O molecule. On dehydrated (100) in liquid paraffin, only one water molecule is necessary to achieve an OH coverage of 4.3OH nm^{-2}. Water is adsorbed by dissociative adsorption on the Al1 site while the dissociated hydrogen group moves to the O1 site (for details sees ref [27]). Compared with the relaxed dehydrated (100) surface, water adsorption results in serious surface reconstruction brought about by O1 and Al2 bond breakage.

DME formation on dehydrated γ-Al_2O_3 in liquid paraffin

In our previous study, there are three possible paths of DME synthesis [14]: Path I, CH_3OH is nondissociative adsorption, and DME is synthesized from two adsorbed CH_3OH; Path II, DME is syntheisized from one adsorbed CH_3OH and one adsorbed CH_3O group; Path III, DME is syntheisized from two adsorbed CH_3O groups. According to these paths, the DME synthesized is studied.

The energy profile of methanol dehydrogenation and the corresponding geometrical transition state on dehydrated γ-

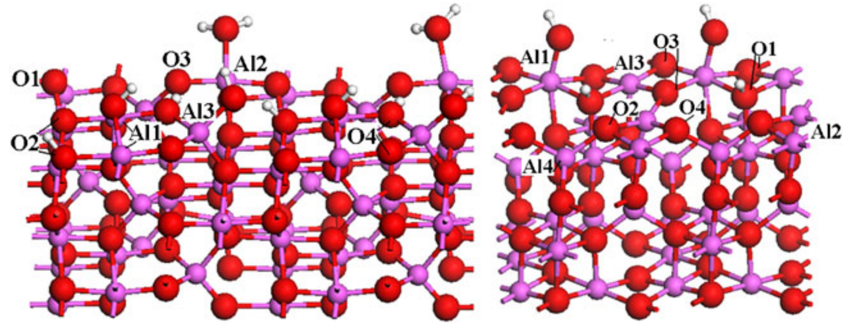

Fig. 2 Side views of the hydrated γ-Al_2O_3(110) (*left*) and (100) (*right*) in liquid paraffin. *Light gray*, *gray* and *white spheres* represent Al, O and H, respectively

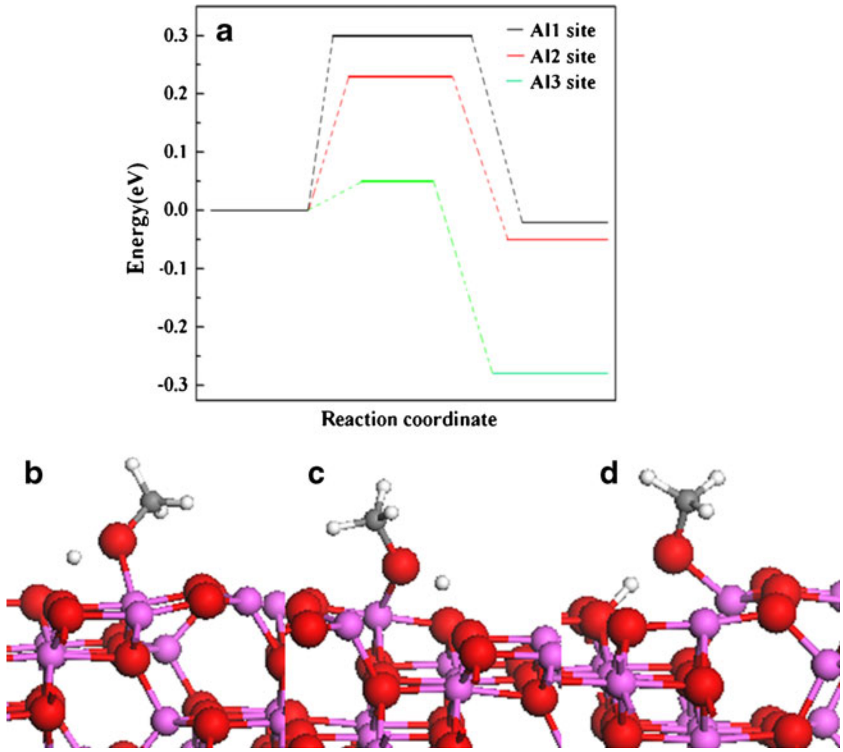

Fig. 3 Energy profile of methanol dehydrogenation on dehydrated (110) in liquid paraffin and transition state(TS) structures. **a** Energy profile. **b**, **c**, **d** TS of methanol dehydrogenation on Al1, Al2 and Al3 sites. *Pink*, *red*, *gray*, and *white spheres* represent Al, O, C, and H atoms, respectively

Al_2O_3 (110) in liquid paraffin are shown in Fig. 3. The activation energies of methanol dehydrogenation, which cause the formation of H and CH_3O groups at the Al1, Al2, and Al3 sites, were 0.30, 0.23, and 0.05 eV, indicating the dissociative adsorption of methanol at typical catalytic conditions (e.g., 280 °C). A small amount of CH_3OH is present due to CH_3OH is dissociative adsorption, and it is impossible that the path I and II occur (for details see ref [14]).

In path III, when two CH_3O groups are co-adsorbed on the Al2 and Al3 sites, the activation energy of the DME synthesis is 1.23 eV and the process of DME synthesis from the two CH_3O groups is endothermic (ΔH=0.82 eV). When two CH_3O groups are co-adsorbed on the Al1 and Al2 sites, the activation energy of DME synthesis is 1.58 eV and the process of DME synthesis from the two CH_3O groups is endothermic (ΔH= 0.61 eV). The energy profile of DME synthesis from two CH_3O groups and the corresponding geometrical transition state are shown in Fig. 4. The stability and activation energy of DME synthesis on the Al1 and Al2 sites were higher than those on the Al2 and Al3 sites by 0.21 eV and 0.35 eV, respectively. These results show that the Al2 and Al3 sites are suitable for DME synthesis, with an activation energy of 1.23 eV.

Methanol dehydrogenation was also studied on the dehydrated γ-Al_2O_3(100) in liquid paraffin. The energy profile of methanol dehydrogenation and the corresponding geometrical transition state are shown in Fig. 5. The activation energies of methanol dehydrogenation for the formation H and CH_3O groups on the Al1, Al2, and Al3 sites were 0.33,

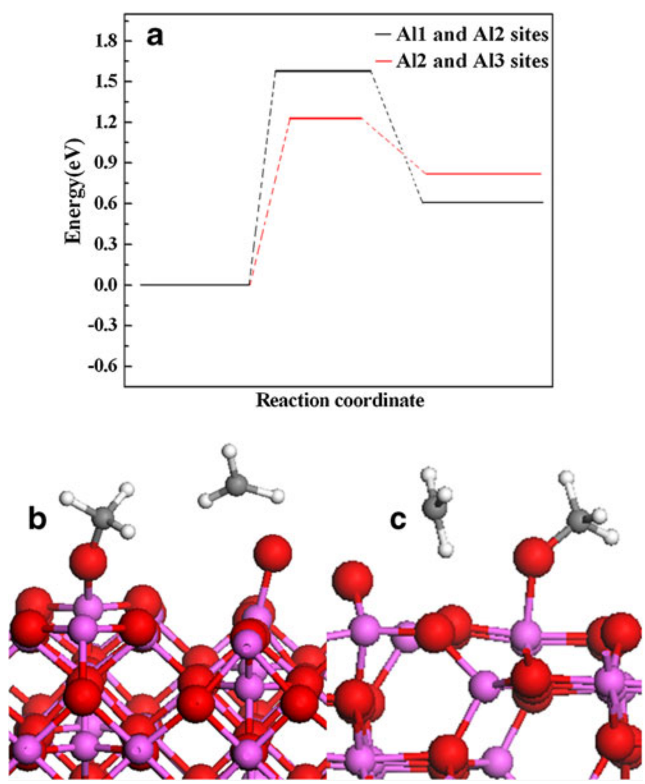

Fig. 4 Energy profile of DME over dehydrated (110) in liquid paraffin and TS structures. **a** Energy profile. **b**, **c** TS of DME synthesis from two adsorbed CH_3O groups over Al1, Al2 and Al2, Al3 sites. The interpretation to color in this figure is referred to the Fig. 3

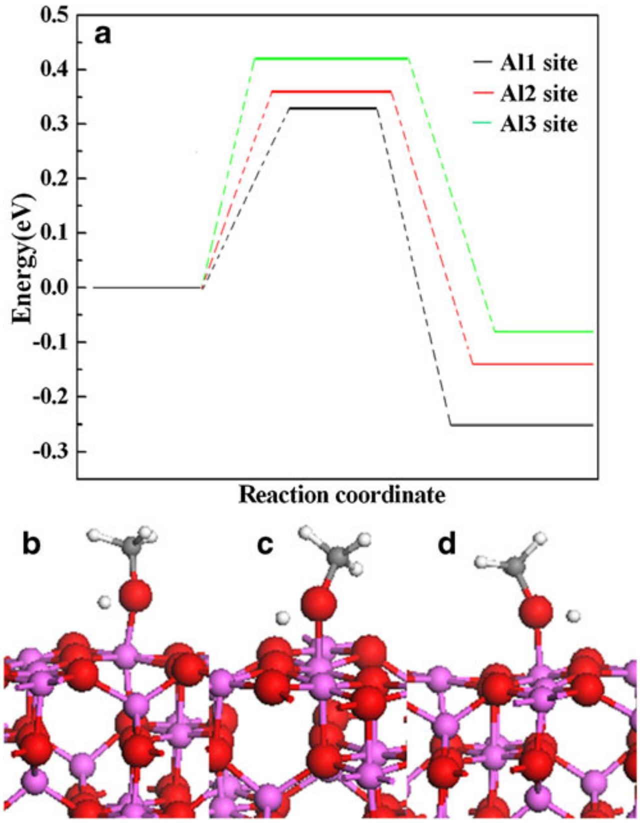

Fig. 5 Energy profile of methanol dehydrogenation on dehydrated (100) in liquid paraffin and TS structures. **a** Energy profile. **b**, **c**, **d** TS of methanol dehydrogenation over Al1, Al2 and Al3 sites. The interpretation to color in this figure is the same as Fig. 3

0.36, and 0.42 eV, respectively. The small activation energies of methanol dehydrogenation also indicate the dissociative adsorption of methanol such that paths I and II cannot occur.

In path III, when two CH_3O groups are co-adsorbed on the Al1 and Al2 sites, the activation energy of DME synthesis is 1.42 eV and the process of DME synthesis from the two CH_3O groups is endothermic ($\Delta H=1.01$ eV). When two CH_3O group molecules are co-adsorbed on the Al2 and Al3 sites, the activation energy of DME synthesis is 1.60 eV, and the process of DME synthesis from the two CH_3O groups is endothermic ($\Delta H=1.28$ eV). The energy profile of DME synthesis from the two CH_3O groups and the corresponding geometrical transition state are shown in Fig. 6. The stability of DME synthesis at the Al1 and Al2 sites was higher than that at the Al2 and Al3 sites by 0.17 eV, but the activation energy of DME synthesis at the Al1 and Al2 sites was lower than that at the Al2 and Al3 sites by 0.18 eV. These results show that the Al1 and Al2 sites are suitable for DME synthesis, with an activation energy of 1.42 eV.

DME formation on hydrated γ-Al_2O_3 in liquid paraffin

On hydrated γ-Al_2O_3(110) in liquid paraffin, only the Al1 and Al2 sites were considered because the Al3 site was unavailable

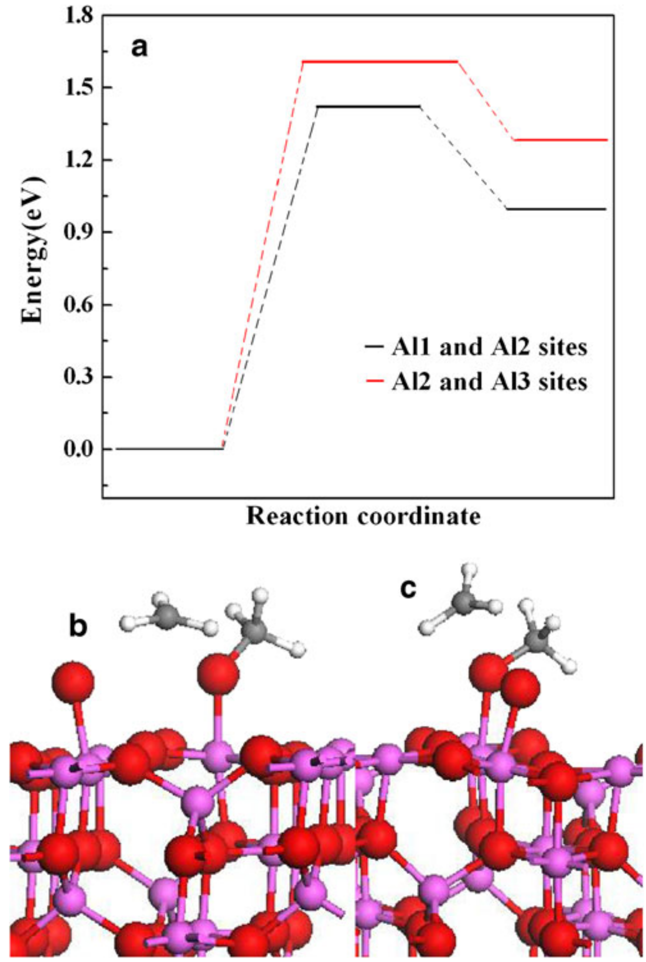

Fig. 6 Energy profile of DME synthesis on dehydrated (100) in liquid paraffin and TS structures. **a** Energy profile. **b**, **c** TS of DME synthesis from two adsorbed CH_3O groups over Al1, Al2 and Al2, Al3 sites. The interpretation to color in this figure is the same as Fig. 3

for adsorption. The activation energies of methanol dehydrogenation for the formation of H and CH_3O groups on the Al1 and Al2 sites were 0.55 and 0.76 eV, respectively (Fig. 7). Compared with the same adsorption sites on the dehydrated (110) in liquid paraffin, the activation energies of methanol dehydrogenation (Al1 and Al2 sites) on the hydrated surface increase. These results show that the adsorption of the OH group or H_2O on the (110) surface restrains methanol dehydrogenation. Thus, paths I and II were considered in this section.

The energy profile of DME synthesis from the two CH_3O groups and the corresponding geometrical transition state are shown in Fig. 8. When two CH_3OH molecules were adsorbed on the Al1 and Al2 sites, the activation energy of DME synthesis from the two adsorbed CH_3OH was 1.11 eV in path I. In path II, the activation energy of DME synthesis from one adsorbed CH_3O group and another adsorbed CH_3OH was 1.02 eV. In path III, the activation energy of DME synthesis from two adsorbed CH_3O group was 1.34 eV. The results show that the activation energy of methanol dehydrogenation

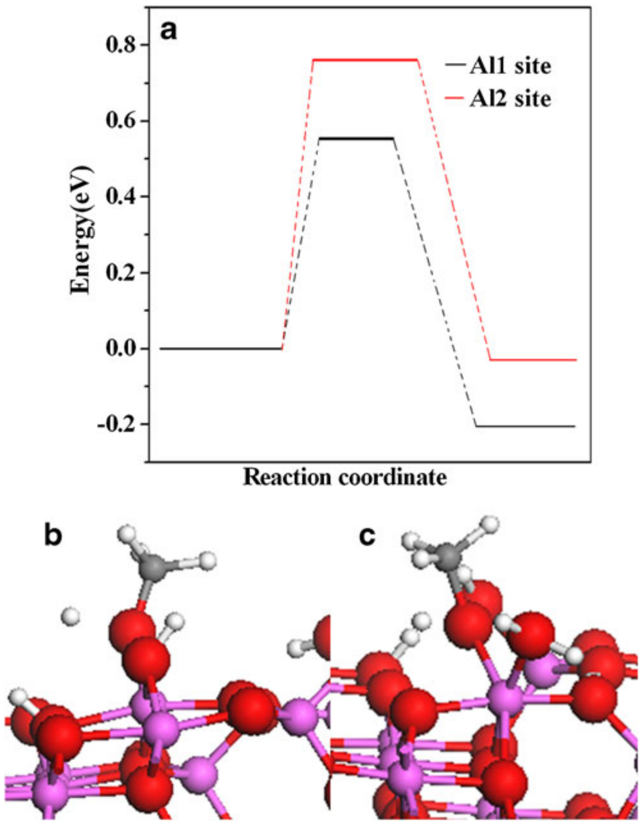

Fig. 7 Energy profile of methanol dehydrogenation on hydrated (110) in liquid paraffin and TS structures. **a** Energy profile. **b**, **c** TS of methanol dehydrogenation on Al1 and Al2 sites. The interpretation to color in this figure is the same as Fig. 3

(0.73 eV) is obviously lower than that of DME synthesis from one methanol and another adsorbed CH_3OH/CH_3O group (1.11/1.02 eV). This behavior indicates that methanol dehydrogenation is preferred over the methanol reaction, in the presence of another adsorbed CH_3OH/CH_3O group. Hence, on hydrated γ-Al_2O_3 (110) in liquid paraffin, DME is formed from two adsorbed CH_3O groups, with an activation energy of 1.34 eV, which is lower than that at the same active sites before hydration of the surface(1.58 eV).

On the hydrated γ-Al_2O_3(100) in liquid paraffin, only the Al2 and Al3 sites were considered because the Al1 site was unavailable for adsorption. Path I cannot occur because methanol adsorption on the Al3 site proceeds through dissociative adsorption. On the Al2 site, the activation energies of methanol dehydrogenation for the formation of H and CH_3O groups on the Al2 site was 0.27 eV, lower than that at the Al2 site on the dehydrated (100) surface (0.36 eV). The transition state is shown in Fig. 9a. The findings indicate that adsorption of an OH group on the (100) surface will accelerate methanol dehydrogenation and that the trend is different on the γ-Al_2O_3(110) surface before and after hydration. Hence, DME synthesis is mainly formed according to path III at an activation energy of 1.45 eV, which is lower than that of the dehydrated (100) surface (1.60 eV). The transition state is shown in Fig. 9b. Comparing the activation energies of DME synthesis on the Al1 and Al2, Al2 and Al3 sites on the (110) and (100) surfaces before and after hydration, it is found that the activation energies after hydration are lower than that of before hydration. In general, as the coordination number of the Al atoms decreases, the Lewis acidity of the Al site becomes strong. This result indicates no close correlation

Fig. 8 Energy profile of DME synthesis on Al1 and Al2 on the hydrated (110) in liquid paraffin and TS structures. **a** Energy profile. **b**, **c**, **d** TS of DME synthesis from two adsorbed CH_3OH groups, one CH_3OH group and one CH_3O group, and two adsorbed CH_3O groups. The interpretation to color in this figure is the same as Fig. 3

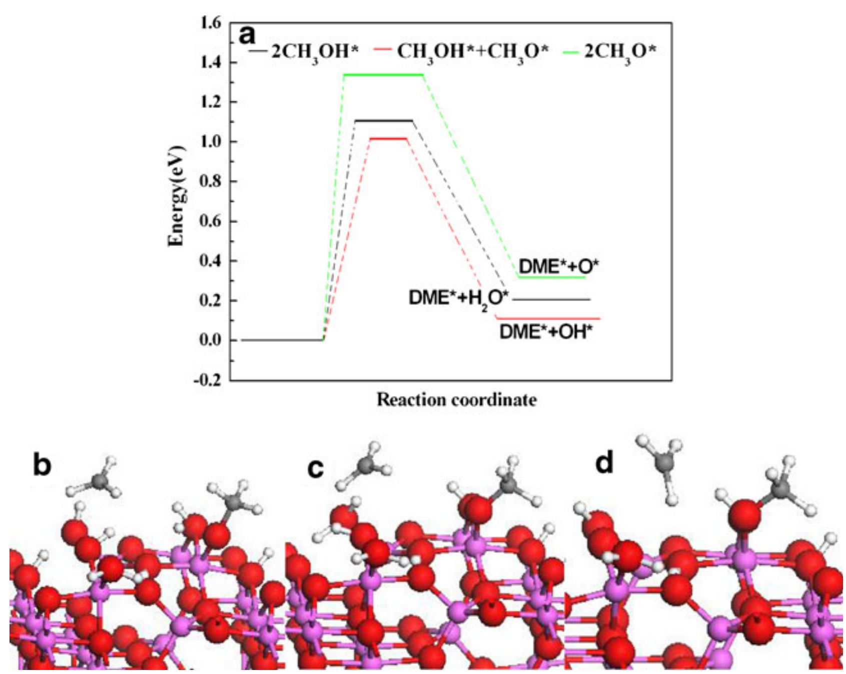

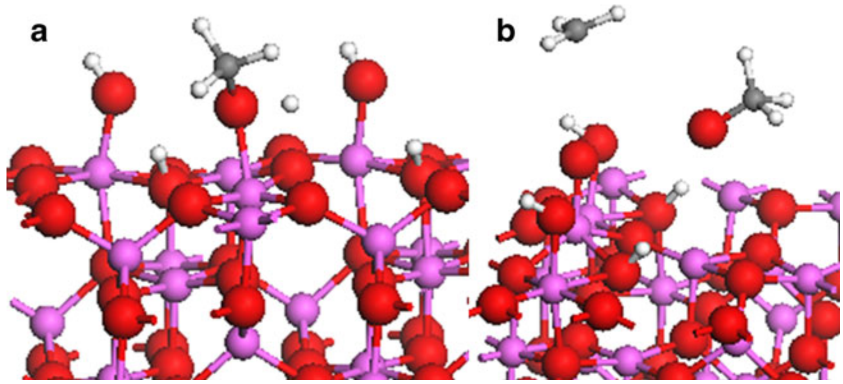

Fig. 9 TS structures on Al1 and Al2 on the hydrated (110) in liquid paraffin. **a** TS structures of methanol dehydrogenation on the Al2 site, **b** DME synthesis on Al3 and Al2 sites on the hydrated (110) in liquid paraffin. The interpretation to color in this figure is the same as Fig. 3

between catalytic activity and acid intensity, consistent with the results obtained by Sung et al. [51], who showed that catalytic activity and number of strong acid sites are not correlated.

Finally, the barrier of the rate-limiting step of DME synthesis from methanol dehydration on γ-Al_2O_3 (110) and (100) in liquid paraffin before and after hydration was considered. The barriers of the rate-limiting step of DME synthesis on dehydrated γ-Al_2O_3 (110) and (100) in liquid paraffin were 1.23 and 1.42 eV, respectively. The barriers of the rate-limiting step of DME synthesis on hydrated γ-Al_2O_3 (110) and (100) in liquid paraffin were 1.34 and 1.45 eV, respectively. The barriers of the rate-limiting step of DME synthesis on the (110) surface were similar before and after hydration (1.42 eV vs. 1.45 eV). However, the barrier of the rate-limiting step of DME synthesis on dehydrated γ-Al_2O_3 (110) in liquid paraffin was lower than that on hydrated γ-Al_2O_3 (110) in liquid paraffin. Assuming the same pre-exponential factor for the reactions at all Lewis acid sites of the γ-Al_2O_3 (110) or (100) in liquid paraffin and using the Arrhenius rate expression $k = Ae^{-E_a/RT}$ [52], the differences in activation energies show DME synthesis rate on dehydrated γ-Al_2O_3 (110) surface in liquid paraffin are faster than 11 times on hydrated γ-Al_2O_3 (110) surface in liquid paraffin at typical catalytic conditions (e.g., 553 K). The results are consistent with the experiment, which indicates the catalytic activity of γ-Al_2O_3 for DME synthesis decreases mainly due to water adsorption [15, 16]. Al3 and Al1 sites on the γ-Al_2O_3 (110) and (100) in liquid paraffin were unavailable for methanol adsorption, and then the catalytic activity further decreases. Considering the area of the (110) and (100) surfaces in actual conditions, the (110) surface predominates 83 % of the total area whereas the (100) surface takes up about 17 %, indicating that Al3 sites on the γ-Al_2O_3 (110) in liquid paraffin dominated during DME synthesis. Catalytic activity decreases mainly because Al3 sites of the (110) surface gradually become inactive. These findings are consistent with the experimental result showing that catalytic activity is also closely related to the fraction of the tetrahedral aluminum sites (Al3 site in our article) [51], which the reaction rate for methanol dehydration decreases about 6–7 times if the fraction of Al3 sites decreases from 0.26 to 0.12. Hence, to prevent γ-Al_2O_3 catalyst deactivation, reductions in the adsorption ability of water on the catalyst surface must be performed by increasing the hydrophobic nature of the surface, such as using different surfactants.

Conclusions

DME synthesis from methanol dehydration on γ-Al_2O_3 (110) and (100) in liquid paraffin before and after hydration was studied by DFT. The calculation results show that DME is mainly formed from two adsorbed CH_3O groups via methanol dehydrogenation before and after hydration. No close correlation was observed between catalytic activity and acid intensity. The barrier for the rate-limiting step of DME synthesis on the (110) surface increase 0.11 eV before and after water adsorption, corresponding to reaction rates of about 11 times slower (T=553 K); the barrier for the rate-limiting step of DME synthesis on the (100) surface before and after water adsorption is similar with each other. This result shows that γ-Al_2O_3 becomes inactive due to water adsorption. Considering the area of the (110) and (100) surfaces under actual conditions, the catalytic activity decreased mainly because the Al3 sites on the (110) surface gradually become inactive. Therefore, to prevent deactivation of the γ-Al_2O_3 catalyst, reductions in the adsorption ability of water on the catalyst surface must be formed by increasing the hydrophobic nature of the surface.

Acknowledgments The authors gratefully acknowledge the financial support of this study by the National Natural Science Foundation of China (Grant No.20676087), China Postdoctoral Science Foundation Funded Project (Grant No.2012M510784), Shanxi Province Science Foundation for Youths (Grant No.012021005-1), Natural Science Foundation of Shanxi Province (Grant No. 2012011046–1), Special/Youth Foundation of Taiyuan University of Technology (No. 2012L042). The authors especially thank for two anonymous reviewers for their valuable suggestions on the quality improvement of our present paper.

References

1. Pan YX, Liu CJ (2007) DFT study on pathways of partial oxidation of DME under cold plasma conditions. Fuel Process Technol 88: 967–976
2. Naik SP, Ryu T, Bui V, Miller JD, Drinnan NB, Zmierczak W (2011) Synthesis of DME from CO_2/H_2 gas mixture. Chem Eng J 167:362–368
3. Baltes C, Vukojević S, Schüth F (2008) Correlations between synthesis, precursor, and catalyst structure and activity of a large set of $CuO/ZnO/ZnO/Al_2O_3$ catalysts for methanol synthesis. J Catal 258: 334–344
4. Flores JH, Peixoto DPB, Appel LG, de Avillez RR, Pais da Silva MI (2011) The influence of different methanol synthesis catalysts on direct synthesis of DME from syngas. Catal Today 172:218–225
5. Abu-Dahrieh J, Rooney D, Goguet A, Saih Y (2012) Activity and deactivation studies for direct dimethyl ether synthesis using CuO–ZnO–Al_2O_3 with NH_4ZSM-5, HZSM-5 or γ-Al_2O_3. Chem Eng J 203:201–211
6. Breman BB, Beenackers AACM, Schuurman HA, Oesterholt E (1995) Kinetics of the gas-slurry methanol-higher alcohol synthesis from $CO/CO_2/H_2$ over a $Cs/Cu/ZnO/Al_2O_3$ catalyst, including simultaneous formation of methyl esters and hydrocarbons. Catal Today 24:5–14
7. Yang RQ, Yu XC, Zhang Y, Li WZ, Tsubaki N (2008) A new method of low-temperature methanol synthesis on $Cu/ZnO/Al_2O_3$ catalysts from $CO/CO_2/H_2$. Fuel 87:443–450
8. Suh YW, Moon SH, Rhee HK (2000) Active sites in $Cu/ZnO/ZrO_2$ catalysts for methanol synthesis from CO/H_2. Catal Today 63:447–452
9. Li J, Zhang QJ, Long X, Qi P, Liu ZT, Liu ZW (2012) Hydrogen production for fuel cells via steam reforming of dimethyl ether over commercial $Cu/ZnO/Al_2O_3$ and zeolite. Chem Eng J 187:299–305
10. Fan JC, Chen CQ, Zhao J, Huang W, Xie KC (2010) Effect of surfactant on structure and performance of catalysts for DME synthesis in slurry bed. Fuel Process Technol 91:414–418
11. Gao ZH, Hao LF, Huang W, Xie KC (2005) A novel liquid-phase technology for the preparation of slurry catalysts. Catal Lett 102:139–141
12. Jain JR, Pillai CN (1967) Catalytic dehydration of alcohols over alumina: mechanism of ether formation. J Catal 9:322–330
13. Schiffino RS, Merrill RP (1993) A mechanistic study of the methanol dehydration reaction on γ-alumina catalyst. J Phys Chem 97:6425–6435
14. Zuo ZJ, Huang W, Han PD, Gao ZH, Li Z (2011) Theoretical studies on the reaction mechanisms of AlOOH- and γ-Al_2O_3-catalysed methanol dehydration in the gas and liquid phases. Appl Catal A 408:130–136
15. Gayubo AG, Aguayo AT, Morán AL, Olazar M, Bilbao J (2002) Role of water in the kinetic modeling of catalyst deactivation in the MTG process. AIChE J 48:1561–1571
16. Gayubo AG, Eren J, Sierra I, Olazar M, Bilbao J (2005) Deactivation and regeneration of hybrid catalysts in the single-step synthesis of dimethyl ether from syngas and CO. Catal Today 106:265–270
17. Mei D, Ge Q, Kwak JH, Kim DH, Szanyi J, Peden CHF (2008) Adsorption and formation of BaO overlayers on γ-Al_2O_3 surfaces. J Phys Chem C 112:18050–19060
18. Cheng L, Ge Q (2008) Effect of BaO morphology on NO_x abatement: NO_2 interaction with unsupported and γ-Al_2O_3-supported BaO. J Phys Chem C 112:16924–16931
19. Cheng L, Ge Q (2007) Effect of γ-Al_2O_3 substrate on NO_2 interaction with supported BaO clusters. Surf Sci 601:L65–L68
20. Digne M, Sautet P, Raybaud P, Euzen P, Toulhoat H (2004) Use of DFT to achieve a rational understanding of acid–basic properties of γ-alumina surfaces. J Catal 226:54–68
21. Raybaud P, Digne M, Iftimie R, Wellens W, Euzen P, Toulhoat H (2001) Morphology and surface properties of boehmite (γ-AlOOH): a density functional theory study. J Catal 201:236–246
22. Digne M, Raybaud P, Sautet P, Guillaume D, Toulhoat H (2008) Atomic scale insights on chlorinated gamma-alumina surfaces. J Am Chem Soc 130:11030–11039
23. Ionescu A, Allouche A, Aycard JP, Rajzmann M (2002) Structure and stability of aluminum hydroxides: a theoretical study. J Phys Chem B 106:5561–5562
24. Pan YX, Liu CJ, Ge QF (2010) Effect of surface hydroxyls on selective CO_2 hydrogenation over Ni_4/γ-Al_2O_3: a density functional theory study. J Catal 272:227–234
25. Zhang RG, Wang BJ, Liu HY, Ling LX (2011) Effect of surface hydroxyls on CO_2 hydrogenation over Cu/γ-Al_2O_3 catalyst: a theoretical study. J Phys Chem C 115:19811–19818
26. Feng G, Huo CF, Deng CM, Huang L, Li YW, Wang JG, Jiao HJ (2009) Isopropanol adsorption on γ-Al_2O_3 surfaces: a computational study. J Mol Catal A 304:58–64
27. Zuo ZJ, Han PD, Hu JS, Huang W (2012) Effect of surface hydroxyls on DME and methanol adsorption over γ-Al_2O_3 (hkl) surfaces and solvent effects: a density functional theory study. J Mol Model 18: 5107–5111
28. Digne M, Sautet P, Raybaud P, Euzen P, Toulhoat H (2002) Hydroxyl groups on γ-Alumina surfaces: a DFT study. J Catal 211:1–5
29. Jennison DR, Schultz PA, Sullivan JP (2004) Evidence for interstitial hydrogen as the dominant electronic defect in nanometer alumina films. Phys Rev B 69:041405
30. Cai SH, Rashkeev SN, Pantelides ST, Sohlberg K (2002) Atomic scale mechanism of the transformation of γ-alumina to θ-alumina. Phys Rev Lett 89:235501
31. Sohlberg K, Pennycook SJ, Pantelides ST (1999) Hydrogen and the structure of transition aluminas. J Am Chem Soc 121:7493–7499
32. Krokidis X, Raybaud P, Gobichon AE, Rebours B, Euzen P, Toulhoat H (2001) Theoretical study of the dehydration process of boehmite to γ-Alumina. J Phys Chem B 105:5121–5130
33. Nortier P, Fourre P, Mohammed Saad AB, Saur O, Lavalley JC (1990) Effects of crystallinity and morphology on the surface properties of alumina. Appl Catal 61:141–160
34. Szaleniec M, Drzewiecka-Matuszek A, Witko M, Hejduk P (2013) Ammonium adsorption on Brønsted acidic centers on low-index vanadium pentoxide surfaces. J Mol Model. doi:10.1007/s00894-013-1951-4
35. Wang SG, Cao DB, Li YW, Wang JG, Jiao HJ (2005) Chemisorption of CO_2 on the nickel surfaces. J Phys Chem C 109:18956–18963
36. Delley B (1990) An all-electron numerical method for solving the local density functional for polyatomic molecules. J Chem Phys 92: 508–517
37. Delley B (2000) From molecules to solids with the $DMol^3$ approach. J Chem Phys 113:7756–7764
38. Perdew JP, Wang Y (1992) Accurate and simple analytic representation of the electron-gas correlation energy. Phys Rev B 45:13244–13249
39. Hohenberg P, Kohn W (1964) Inhomogeneous electron gas. Phys Rev B 136:864–871
40. Kohn W, Sham LJ (1965) Self-consistent equations including exchange and correlation effects. Phys Rev A 140:1133–1138
41. Zuo ZJ, Sun LL, Huang W, Han PD, Li ZH (2010) Surface properties of copper in different solvent mother solutions: a density functional theory study. Appl Catal A 375:181–187
42. Singh A, Ganguly B (2008) DFT study of urea interaction with potassium chloride surfaces. Mol Simul 34:973–979
43. Zhang RG, Ling LX, Wang BJ (2012) Density functional theory analysis of carbonyl sulfide hydrolysis: effect of solvation and nucleophile variation. J Mol Model 18:1255–1262
44. Mojica ERE (2013) Screening of different computational models for the preparation of sol–gel imprinted materials. J Mol Model. doi:10.1007/s00894-013-1928-3

45. Zuo ZJ, Huang W, Han PD, Li ZH (2010) Solvent effects for CO and H_2 adsorption on Cu_2O (1 1 1) surface: a density functional theory study. Appl Surf Sci 256:2357–2362
46. Halgren TA, Lipscomb WN (1977) The synchronous-transit method for determining reaction pathways and locating molecular transition states. Chem Phys Lett 49:225–232
47. Wang SG, Liao XY, Hu J, Cao DB, Li YW, Wang JG, Jiao HJ (2007) Kinetic aspect of CO_2 reforming of CH_4 on Ni(1 1 1): a density functional theory calculation. Surf Sci 601:1271–1284
48. Maresca O, Allouche A, Aycard JP, Rajzmann M, Clemendot S, Hutschka F (2000) Quantum study of the active sites of the γ-alumina surface: chemisorption and adsorption of water, hydrogen sulfide and carbon monoxide on aluminum and oxygen sites. J Mol Struct THEOCHEM 505:81–94
49. Maresca O, Ionescu A, Allouchea A, Aycard JP, Rajzmann M, Hutschka F (2003) Quantum study of the active sites of the γ alumina surface (II): QM/MM (LSCF) approach to water, hydrogen disulfide and carbon monoxide adsorption. J Mol Struct THEOCHEM 620: 119–128
50. Arrouvel C, Toulhoat H, Breysse M, Raybaud P (2004) Effects of P_{H2O}, P_{H2S}, P_{H2} on the surface properties of anatase-TiO_2 and γ-Al_2O_3: a DFT study. J Catal 226:260–270
51. Sung DM, Kim YH, Park ED, Yie JE (2012) Role of surface hydrophilicity of alumina in methanol dehydration. Catal Commun 20:63–67
52. Yang YX, Evans J, Rodriguez JZ, White MG, Liu P (2010) Fundamental studies of methanol synthesis from CO_2 hydrogenation on Cu(111), Cu clusters, and Cu/ZnO(0001). Phys Chem Chem Phys 12: 9909–9917